Modeling and Hybrid Control of a Constrained Rigid Robotic System

Amine CHAÂBOUNI, Ines BELAÏD DLIMI and Hichem KALLEL

PhD student in Electrical Engineering, Department of Physics and Electrical Engineering, National Institute of Applied Science and of Technology, INSAT, Centre Urbain Nord BP 676 - 1080 Tunis Cedex, Tunisia

chaabouni.amine@gmail.com, inesdlimi@gmail.com, golden.k@gnet.tn

Abstract

In this paper, a nonlinear hybrid position/force control is designed for a constrained two degrees of freedom robot. System dynamics is formulated based on Lagrange-Euler approach. Our objective is to control separately the movement of the robot and its contact forces. The contact force is obtained via the inverse dynamics with dynamic frictional force. Force control is realized through a virtual desired position of the end effector. Simulation results give satisfactory outcomes and proof the efficiency of the proposed hybrid control concept.

Keywords: *hybrid control; force control; constrained robot manipulators; contact force modeling*

1. Introduction

Manipulator robots are widely used in industry due to their flexibility, dexterity and precision. Most Robot tasks involve contact with its environment. In order to achieve such tasks, the manipulator robot not only must perform the desired motion but also controls continuously the forces exerted on its surrounding. Such motion involves friction contact forces. There are several classical models in the literature describing the friction forces [8].

The forces exerted by the robot on its environment and its motion must be controlled separately. Hybrid force/position control concept is pertinent in such tasks, involving constrained robots performing a motion.

Robert and Craig [6, 7] introduced the force control concept through a hybrid control design, in the 80's. Since then, many authors have contributed in this field, such as J.K. Mills and A.A. Goldenberg [9] who achieved a contact force and position control of a manipulator's end-effector during constrained motion tasks; their proposed method exploits the fundamental structure of the manipulator's constrained motion dynamics formulation. An overview of robot force control is presented in G. Zeng and A. Hemami [2].

In this work, a nonlinear hybrid control of two degrees of freedom constrained manipulator is achieved. The robot's end effector is in continuous contact with a rigid surface, exerting on it a normal force while realizing a sliding motion. Frictional forces are present during the sliding motion.

The paper is organized as follows: We first introduce the constrained system dynamic of a tow degrees of freed robot. An analysis of the contact forces and their relation with the movement of the end effector is performed in order to impose a desired virtual dynamics. Consequently, a hybrid position/force control is proposed to realize not only the desired movement but also the desired contact force.

2. Dynamics' Model of the Constrained Robotic System

This robotic system (Figure 1) is an arm manipulator with two degrees of freedom. It consists of two rigid bodies (***b₁*** and ***b₂***) interconnected by revolute links and equipped with two ideal motors (***M₁* and *M₂***) at the joints. At the end effector, a weight $\boldsymbol{m_3}$ is fixed to the second element $\boldsymbol{b_2}$. This weight is used to analyze the dynamics of the end effector.

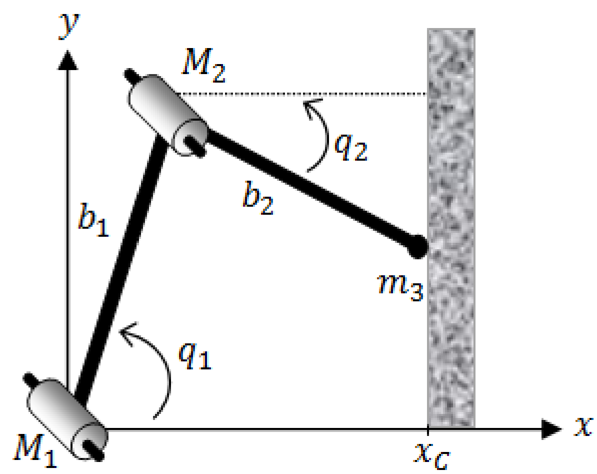

Figure 1. Diagram of the Constrained Robot

We define by $q = [q_1 \quad q_2]^T \in \mathcal{R}^{nx1}$ the angular positions' vector of the robot, l_i the length of the rigid body b_i, k_i the gravity's center of b_i, m_i the mass of the ith element of the robot, and x_C coordinate of the contact surface on the horizontal axis (***x*** axis),.

The motion of the robot's is defined by $\boldsymbol{x_i}$ which is the center of gravity's position of the i^{th} element of the robot along the normal (horizontal) axis ***x*** and $\boldsymbol{y_i}$ which is the center of gravity's position of the i^{th} element of the robot along the tangential (vertical) axis ***y***.

The dynamics' model as follow:

$$\boldsymbol{J(q)\ddot{q} + H(q,\dot{q}) + G(q) + \frac{\partial C_x}{\partial q}^T F_N + \frac{\partial C_y}{\partial q}^T F_T = DU} \tag{2-1}$$

The used matrices in this equation are defined and detailed in Appendix A.

We define by F_N the normal force applied by the robot's end effector on the contact surface. This normal force is generated by the robot to exert a desired contact force by the end effector on the contact surface. F_T is the tangential force applied by the robot's end effector along the ***y*** axis of the contact surface. This tangential contact force is generated by the robot to realize a sliding movement by the end effector vertically along the contact surface.

3. Dynamics of the End Effector

To fully determine the dynamic model of constrained robot, its interaction with the environment must be totally defined. Thus, the three following hypothesis were considered:

- Hypothesis 1: The contact between the robot's end effector and the rigid contact surface is continuously maintained.
- Hypothesis 2: The robot's end effector cannot exceed the rigid contact surface.
- Hypothesis 3: The robot's end effector is free to move vertically along the contact surface with press of friction.

In fact, our objective is to move the robot's end effector along the contact surface (to a desired position y_d) while exerting a desired normal force. Such task retains only one degree freedom. Frictional force is present due to contact nature.

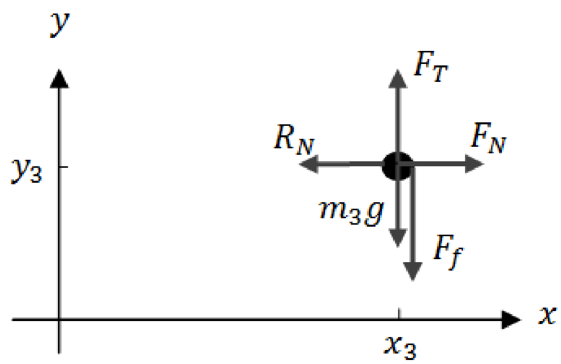

Figure 2. Results of the applied forces to the robot's end effector m_3

We define by R_N the normal reaction force applied by the contact surface on the robot along the ***x*** axis, and F_f the friction force which is a tangential reaction applied by the contact surface on the robot.

To calculate the constrained forces, an analysis of the dynamic of the end effector is presented here:

3.1. Contact Force Projections

The applied forces through the normal contact surface's axe $\vec{x}$ are defined by

$$m_3\overrightarrow{\ddot{x}_3} = \overrightarrow{F_N} - \overrightarrow{R_N} = 0 \tag{3-2}$$

Along the tangential contact surface's axe $\vec{y}$, the applied forces' are as follow:

$$m_3\overrightarrow{\ddot{y}_3} = \overrightarrow{F_T} - m_3\vec{g} - \overrightarrow{F_f} \tag{3-3}$$

3.2. Normal Contact Force's Formulation

To ensure the hypothesis above, the robot is always in contact with the contact surface and can in no case exceed it; the coordinate of the end effector x_3 along the normal axis to the contact surface x does not vary, thus,

$$\begin{cases} x_3 = x_C \\ \dot{x}_3 = 0 \\ \ddot{x}_3 = 0 \end{cases} \tag{3-4}$$

In appendix B we deduct that the normal reaction R_N can be written as:

$$R_N = g_1(q,\dot{q}) + g_2(q)U = F_N \tag{3-5}$$

3.3. Frictional Force Modeling

The surface friction form F_f is modeled as presented by Figure 3. Its magnitude depends on the surface nature and the speed of the end effector along the movement.

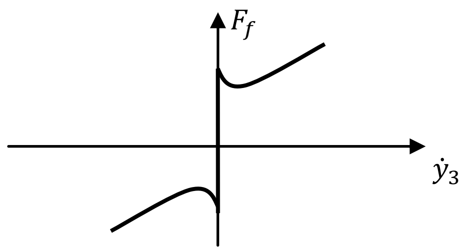

Figure 3. Frictional force model: Coulomb + viscous + static friction +Stribeck effect

We assume that our robot operates under variable charges. The frictional force depends on both the end effector velocity ($\dot{y}_3$) and charge (Γ_N), such as:

$$F_f = F_f(\dot{y}_3, \Gamma_N) \tag{3-6}$$

These choices give the following model of the frictional force:

$$\begin{cases} F_f = (F_{cou} + F_{vis} + (F_s - F_c)\left(exp\left|\frac{\dot{y}_3}{v_s}\right|^{\gamma_s}\right) sign(\dot{y}_3))\frac{\Gamma_N}{\Gamma_0} \\ F_{cou} = F_c\, sign(\dot{y}_3) \\ F_{vis} = F_v\, \dot{y}_3 \end{cases} \tag{3-7}$$

The definition of the frictional force's variables is given in the appendix C.

4. Constrained Robot's Hybrid Control

The control objective is to move the robot's end effector vertically along the contact surface to a desired position y_{3d} while exerting on it a normal contact force F_{Nd}.

To realize such objective, the end effector's motion task and the normal force are controlled separately. The desired dynamics of the end effector is a follow:

- A **normal** desired motion of the end effector, considering the desired normal contact force $\boldsymbol{F_{Nd}}$:

$$m_3\ddot{x}_{3_d} = F_N - F_{Nd} \tag{4-8}$$

Note that $\boldsymbol{x_{3d}}$ is a virtual displacement of the end effector inside the contact surface: the dynamics of $\boldsymbol{x_{3d}}$ defines the desired response of the normal contact force F_N. We define F_{Nd} as the desired normal force.

- A **tangential** desired motion of the end effector, considering the desired tangential contact force $\boldsymbol{F_{T_d}}$:

$$m_3\ddot{y}_{3d} = F_T - F_{Td} \tag{4-9}$$

We define $\mathrm{F_{Td}}$ as the desired tangential force.

The control strategy is based on a virtual reference model of the end effector's desired dynamics, in order to reach the control's objective defined above. The reference model is given by the differential equations below:

- A **virtual** reference model for the contact force regulation:

$$\ddot{x}_{3_d} - \Lambda_3\dot{x}_{3_d} - \Lambda_4\left(x_{3_d} - x_3\right) = 0 \tag{4-10}$$

- A motion regulator's reference model:

$$\left(\ddot{y}_{3_d} - \ddot{y}_3\right) - \Lambda_1\left(\dot{y}_{3_d} - \dot{y}_3\right) - \Lambda_2\left(y_{3_d} - y_3\right) = 0 \tag{4-11}$$

Here, the weighting matrices ($\Lambda_1$and Λ_2) and the virtual weighting matrices ($\Lambda_3$and Λ_4) are negative definite (see Appendix D).

If the desired motion dynamics is satisfied, then we insure that the tangential contact force $\mathrm{F_T}$ tends to the desired value $\mathrm{F}_{\boldsymbol{Td}}$ and the normal force $\mathrm{F_N}$ equals to the desired value $\mathrm{F}_{\mathrm{N}\boldsymbol{d}}$.

4.1. Position Control

The position control's objective is to make the robot's end effector move upward then down along the contact surface, independently of the normal contact force exerted on it.

This objective is realized by controlling to the tangential applied forces to the robot's end effector:

$$m_3\overrightarrow{\ddot{y}_3} = \overrightarrow{F_T} - \left(\overrightarrow{F_f} + m_3\vec{g}\right) \tag{4-12}$$

Using the decoupling nonlinear control defined above (4-4) by the motion reference model, the desired tangential force expressed in (4-2) is obtained:

$$F_{Td} = \left(m_3 g + F_f\right) - m_3\left(\Lambda_1\left(\dot{y}_{3_d} - \dot{y}_3\right) + \Lambda_2\left(y_{3_d} - y_3\right)\right) \tag{4-13}$$

The position's control of the robot is realized with a position's regulator that can be expressed as follows:

$$U_T = \frac{\boldsymbol{\partial C_y}^{\boldsymbol{T}}}{\boldsymbol{\partial q}}\; m_3\left(\Lambda_1\left(\dot{y}_{3_d} - \dot{y}_3\right) + \Lambda_2\left(y_{3_d} - y_3\right)\right) \tag{4-14}$$

4.2 Force Control

The objective of the force's control is to apply a desired force by the robot's end effector on the contact surface, independently of the motion control. According to the applied forces' normal projection, the contact force is written as follows:

$$m_3\ddot{x}_3 = F_N - R_N \tag{4-15}$$

The virtual system defined in (4-1) is considered in order to make the normal force $\boldsymbol{F_N}$ tend to the desired value $\boldsymbol{F_{Nd}}$.

Considering the desired stable dynamics of $\boldsymbol{x_{3d}}$ (4-3), the second order model insures that $\boldsymbol{x_{3d}}$ tend to the constant value $\boldsymbol{x_3}$ since the surface is non-elastic (rigid), and from the considered virtual system, we achieve that $\boldsymbol{F_N}$ equals the desired normal force $\boldsymbol{F_{Nd}}$.

$$F_N = F_{N_d} - m_3\left(\Lambda_3 \dot{x}_{3_d} + \Lambda_4\left(x_{3_d} - x_3\right)\right) \tag{4-16}$$

Injecting the virtual desired system into the equation of the force's normal projection, the desired velocity has formulated such as:

$$\dot{x}_{3_d} = \left(\frac{1}{m_3}\right)\int\left(F_{N_d} - F_N\right)dt \tag{4-17}$$

The desired position has also expressed, according to the normal contact force, such as:

$$\left(x_{3_d} - x_3\right) = \left(\frac{1}{m_3}\right)\iint\left(F_{N_d} - F_N\right)dt^2 \tag{4-18}$$

So, the contact force's regulator has realized from the equation above and the force's control has computed, such as:

$$U_N = \frac{\partial \boldsymbol{C_x}^{\boldsymbol{T}}}{\partial \boldsymbol{q}}\left(\Lambda_3\int\left(F_{N_d} - F_N\right)dt + \Lambda_4\iint\left(F_{N_d} - F_N\right)dt^2\right) \tag{4-19}$$

4.3 Equilibrium Study

The objective of the equilibrium study is to ensure keeping the robot at the desired position and contact force at the equilibrium state. Two study cases can be considered: the static equilibrium that is maintaining the robotic system stability only when it is stationary and the dynamic equilibrium that maintains the stability even while in motion. We studied and compared these two cases below.

4.3.1. Static Equilibrium: At the equilibrium state, the robot's end effector is kept at the desired position and the desired contact force. The objective of the static equilibrium's study is to ensure keeping the whole robotic system stability when it reaches the equilibrium state. The equilibrium's torque $\mathbf{U_{eq}}$ is written as:

$$U_{eq} = \left.\frac{\partial \boldsymbol{C_x}^{\boldsymbol{T}}}{\partial \boldsymbol{q}}\right|_{q=q_d} F_{Nd} + \left.\frac{\partial \boldsymbol{C_y}^{\boldsymbol{T}}}{\partial \boldsymbol{q}}\right|_{q=q_d} m_3 g + G(q_d) \tag{4-20}$$

- $\left.\frac{\partial \boldsymbol{C_x}^{\boldsymbol{T}}}{\partial \boldsymbol{q}}\right|_{q=q_d} F_{Nd}$: Maintaining the contact force of the robot's end effector.
- $\left.\frac{\partial \boldsymbol{C_y}^{\boldsymbol{T}}}{\partial \boldsymbol{q}}\right|_{q=q_d} m_3 g$: Maintaining the robot's end effector at the desired position.
- $G(q_d)$: Maintaining the robotic system's equilibrium at the desired position.

The disadvantages of this approach are the start's peaks, the fluctuations in the contact force and the necessity of a large torque's gradient. To overcome these disadvantages, the robot dynamic equilibrium has studied below.

4.3.2. Dynamic Equilibrium: The objective of the dynamic equilibrium's study is to ensure keeping the whole robotic system stability even when it is in motion. The torque at the equilibrium is written as follows:

$$U_{eq} = \frac{\partial c_x}{\partial q}^T F_{Nd} + \frac{\partial c_y}{\partial q}^T m_3 g + H(q, \dot{q}) + G(q) \tag{4-21}$$

This dynamic approach improves system performance and provides better stability of the robot.

4.4. Hybrid Position/Force Control Strategy

The diagram below (Figure 4) shows the control's principle applied to the robot.

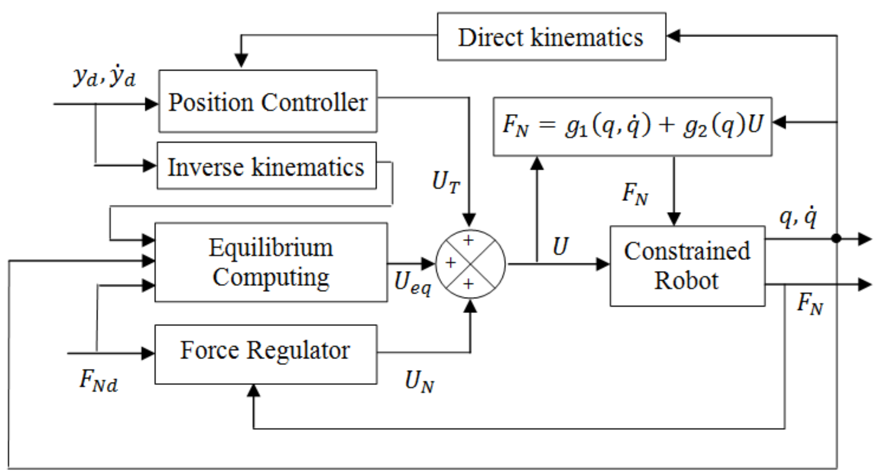

Figure 4. Block Diagram of the Applied Control's Principle

The hybrid position/force control strategy is calculated by an addition of the results of the two regulation's blocks with an equilibrium term to maintain the robotic system stability only at equilibrium's position or even throughout the motion, such as:

$$U = U_N + U_T + U_{eq} \tag{4-22}$$

4.5Stability analysis

For our stability analysis, we have ensured that the robot's end effector is globally stable since (4.3) and (4.4) guarantee the convergence of its coordinates to the desired state.

Since our system is a robot to two freedom degrees and the convergence of the two coordinates ($\boldsymbol{x_3}$ and $\boldsymbol{y_3}$) is guaranteed, therefore the overall global stability is ensured.

The stability proof of the end effector is a follows:

Let e be the vector of position's error defined by:

$$e = \begin{bmatrix} y_{3d} - y_3 \\ \dot{y}_{3d} - \dot{y}_3 \\ x_{3d} - x_3 \\ \dot{x}_{3d} \end{bmatrix} \tag{4-23}$$

Using the reference models' definitions expressed in (4-3) and (4-4), the following time derivative of the position's errors vector describing the error dynamics is given:

$$\dot{\boldsymbol{e}} = \boldsymbol{\Lambda}\, \boldsymbol{e} \tag{4-24}$$

Here $\Lambda \in \mathcal{R}^{2\mathrm{nx}2\mathrm{n}}$ is a matrix negative definite, composed as follows:

$$\Lambda = \begin{bmatrix} 0 & 1 & 0 & 0 \\ \Lambda_2 & \Lambda_1 & 0 & 0 \\ 0 & 0 & 0 & 1 \\ 0 & 0 & \Lambda_4 & \Lambda_3 \end{bmatrix} \tag{4-25}$$

So let's consider the following Lyapunov function:

$$V = \frac{1}{2} e^T M e > 0 \qquad \forall t > 0, \forall e \neq 0 \tag{4-26}$$

Where $\mathrm{M} = \mathrm{M}^\mathrm{T} \in \mathcal{R}^{2\mathrm{nx}2\mathrm{n}}$ and $\mathrm{Q} \in \mathcal{R}^{2\mathrm{nx}2\mathrm{n}}$ are positive definite matrices, given by the following Riccati equation:

$$\mathrm{M}\Lambda + \Lambda^\mathrm{T}\mathrm{M} + \dot{\mathrm{M}} + \mathrm{Q} = 0 \tag{4-27}$$

The time derivative $\dot{\mathrm{V}}$ of Lyapunov function is computed such as:

$$\dot{V} = e^T \left(M\Lambda + \frac{1}{2}\dot{M} \right) e \tag{4-28}$$

Using the Riccati equation written above, the time derivative of Lyapunov function becomes:

$$\dot{V} = e^T \left(-\frac{1}{2} Q \right) e < 0 \qquad \forall t > 0, \forall e \neq 0 \tag{4-29}$$

The time derivative of the Lyapunov function is negative definite since the specified above matrix $\boldsymbol{Q}$ is positive definite. Therefore, the stability of the robot's end effector is guaranteed, generating the overall global stability of the robotic system.

5. Simulation Results and Discussion

In this section, the simulation results of the hybrid force/position control method developed above are applied for the 2 degrees of freedom constrained manipulator.

Throughout the simulation, the robot's end effector is in permanent contact with the rigid surface.

The motion's task is to move the end effector of the manipulator first from $\mathrm{y}_{3\mathrm{i}}$, the initial tangential position of the end effector to y_d=0.7m and from y_d=0.7m to y_d=0.5m second, along the contact surface.

The force's task is to exert a normal contact force, by the robot's end effector, on the rigid contact surface, first from F_{Ni}, the initial normal force of the end effector to F_{Nd}=14N and second from F_N=14N to F_{Nd}=7N.

Table 1. Two Degrees of Freedom Robot's Manipulator with the Hybrid Control

	Hybrid control with static equilibrium	*Hybrid control with dynamic*
Coordinates (m)	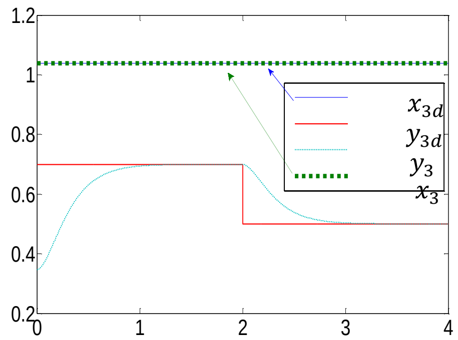	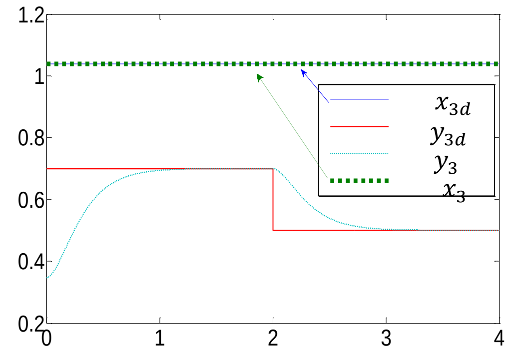
Forces (N)	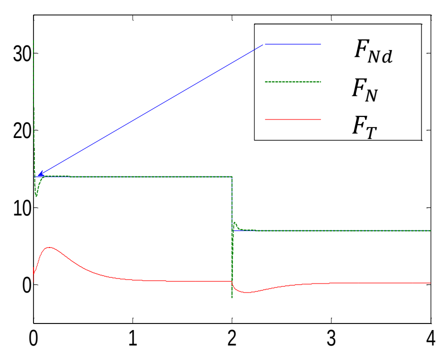	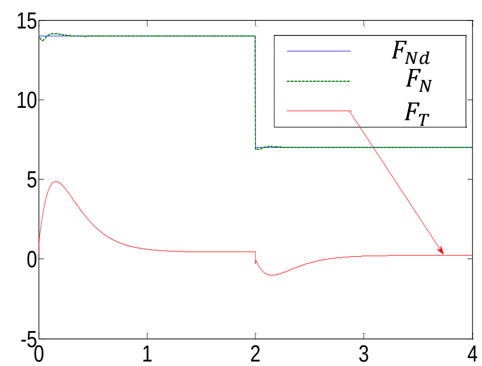
Positions (m)	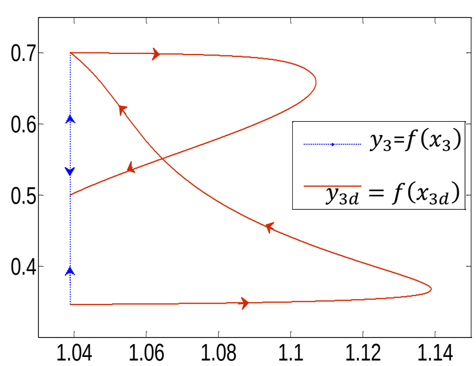	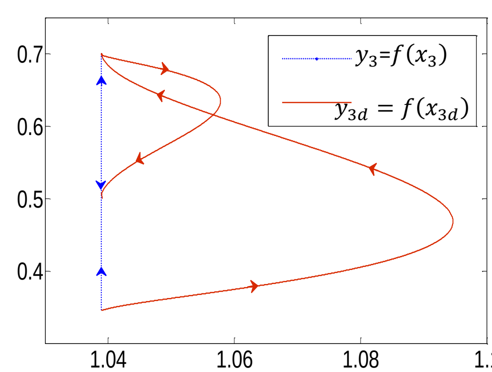
Torques (Nm)	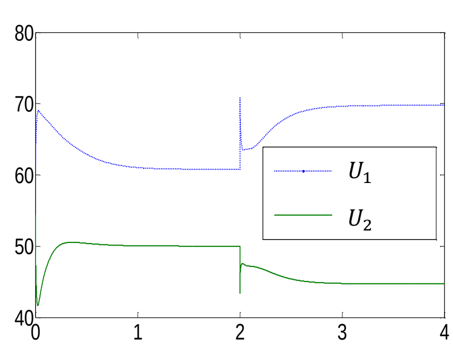	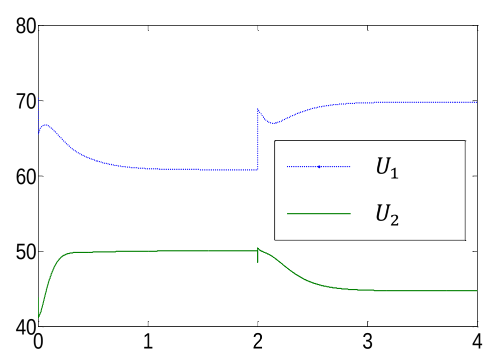

The weighting matrices $\Lambda_1$and Λ_2 and the virtual weighting matrices Λ_3 and Λ_4 are:

$$\begin{cases} \Lambda_1 = \sum_{i=1}^{2} p_i \\ \Lambda_2 = \prod_{i=1}^{2} p_i \\ p_1 = p_2 = -6 \end{cases} \quad \& \quad \begin{cases} \Lambda_3 = \sum_{i=1}^{2} s_i \\ \Lambda_4 = \prod_{i=1}^{2} s_i \\ s_1 = s_2 = -70 \end{cases} \tag{5-1}$$

Tow simulation of this movement are presented in table 1 in which we have used prior the stat equilibrium method and secondly the dynamic method.

Through the simulation results, we observe that the two proposed force/position controllers are capable to stabilize and bring the constrained robotic system to its desired forces and positions. However, the dynamic equilibrium gives less overshooting in the contact force curves and less fluctuations in the control torques then the static equilibrium. The two simulations have approximately the same response time since the desired imposed movement is the same.

Via the simulation results of the force control, we observe that the dynamics of the virtual displacement $\boldsymbol{x_{3d}}$ defines the desired response of the normal contact force $\boldsymbol{F_N}$: More the difference between the virtual displacement $\boldsymbol{x_{3d}}$ and the position of the end effector $\boldsymbol{x_3}$ is large more the difference between the normal force and its desired value is big.

Using the hybrid control with the dynamic equilibrium, we note that the virtual displacement x_{3d} of the end effector on the contact surface is smaller, resulting smaller peaks in the starting forces and the torques applied to the robot.

The hybrid control with the dynamic equilibrium is more compatible with the real applications due to the absence of overshooting in the torque motors.

6. Conclusion

In this paper, we have synthesized a hybrid force/motion control for a two freedom degrees constrained manipulator robot. The robot's end effector is continuously in contact with a rigid contact surface.

The forces exerted by the robot on its environment and its motion are controlled separately, despite the dependency of the contact force exerted by the robot on the rotation angles of its joints. This force and motion decoupling allows flexibility in fixing the two combined controls' parameters independently, and thus a better response time of the desired contact force.

The position control is achieved via a dynamic desired tangential position of the robot end effector. The control force is performed via a dynamic virtual normal position desired of the robot's end effector, because of the permanent contact with the contact surface.

This control is stabilizing taking into account the frictional forces due to the contact maintained during the sliding motion of the robot end effector with the contact surface.

A stability analysis of the end effector was proven based on Lyapunov formulation. Simulation results not only confirm the stability but also showed high performance in term of trajectory trucking. When dynamic equilibrium was used, the necessary torque control was closer to the physical realization.

APPENDIX

Appendix A: *Dynamics' model formulation*

The dynamics' model of the constrained 2 degrees of freedom robot's manipulator is found depending on Lagrange-Euler differentiation:

$$J(q)\ddot{q} + H(q,\dot{q}) + G(q) + {C_x}^T F_N + {C_y}^T F_T = DU \tag{A-1}$$

The matrices used in this equation are defined as follows:

- $J(q) = \begin{bmatrix} \left(m_1{k_1}^2 + (m_2+m_3){l_1}^2 + I_1\right) & l_1\, C_{1-2}(m_2k_2 + m_3l_2) \\ l_1\, C_{1-2}(m_2k_2 + m_3l_2) & \left(m_2{k_2}^2 + m_3{l_2}^2 + I_2\right) \end{bmatrix}$: Inertia matrix.
- $H(q,\dot{q}) = \begin{bmatrix} 0 & l_1S_{1-2}(m_2k_2 + m_3l_2) \\ -l_1S_{1-2}(m_2k_2 + m_3l_2) & 0 \end{bmatrix} \begin{bmatrix} {\dot{q}_1}^2 \\ {\dot{q}_2}^2 \end{bmatrix}$: Coriolis and centrifugal forces vector.
- $G(q) = g\begin{bmatrix} (m_1k_1 + (m_2+m_3)l_1)\, C_1 \\ (m_2k_2 + m_3l_2)\, C_2 \end{bmatrix}$: Gravity vector.
- $g = 9.8062$: gravity constant parameter
- $D = \begin{bmatrix} 1 & -1 \\ 0 & 1 \end{bmatrix}$: transformation matrix
- $I_i,\quad i = (1,2)$: Inertia variable of the i[th] motor (M_i) and the i[th] element of the robot (b_i).
- $C(q) \in \mathcal{R}^{nxp} = \begin{bmatrix} C_x \\ C_y \end{bmatrix} = \begin{bmatrix} x_3 \\ y_3 \end{bmatrix}$: Position's vector of the end effector:
- $F_N \in \mathcal{R}^{1x1}$: Normal contact force exerted by the robot's end effector on the contact surface.
- $F_T \in \mathcal{R}^{1x1}$: Tangential contact force exerted by the robot's end effector along the contact surface.
- $U \in \mathcal{R}^{nx1} = [U_1 \quad U_2]^T$: Vector of torques generated by the robot's motors M_1 and M_2.

Appendix B: *Normal contact force formulation*

Since the robot is continuously in contact with the rigid obstacle and in no case can exceed it, the coordinate of the end effector $\boldsymbol{x_3}$ along the normal axis to the contact surface $\boldsymbol{x}$ does not vary. Thus, its first and second derivatives are nulls. So, the normal acceleration can be expressed as follows:

$$\ddot{x}_3 = \left(\frac{\partial C_x}{\partial q}\dot{q}\right)\dot{q} + C_x\,\ddot{q} = 0 \tag{B-1}$$

By injecting this expression into the dynamics' model of the constrained robot (A-1), the following formulation of the contact forces' vector is found:

$$C_x\, J(q)^{-1} C^T(q)\, F \; = C_x\, J(q)^{-1}\left(DU - H(q,\dot{q}) - G(q)\right) + \left(\frac{\partial C_x}{\partial q}\dot{q}\right)\dot{q}$$

We obtain the following equation, relating the tangential and normal forces:

$$B_1(q)F_N \; + \; B_2(q)F_T = f_1(q,\dot{q}) + f_2(q)U \tag{B-2}$$

This was found using the functions defined below:

$$\begin{cases} B_1(q) = C_x J^{-1} {C_x}^T \\ B_2(q) = C_x J^{-1} {C_y}^T \\ f_1(q,\dot{q}) = -C_x J^{-1} (H+G) - \left(\frac{\partial C_x}{\partial q}\dot{q}\right)\dot{q} \\ f_2(q) = C_x J^{-1} D \end{cases} \tag{B-3}$$

Using the kinematics' modeling of the end effector's accelerations, defined as follows:

$$\begin{cases} \ddot{y_3} = -h_2(q)\,\dot{q}^2 + h_1(q)\ddot{q} \\ \ddot{x_3} = -h_1(q)\,\dot{q}^2 - h_2(q)\,\ddot{q} = 0 \end{cases} \tag{B-4}$$

Here, the used functions are:

$$\begin{cases} h_1(q) = [l_1 C_1 \quad l_2 C_2] \\ h_2(q) = [l_1 S_1 \quad l_2 S_2] \\ \dot{q}^2 = \left[{\dot{q}_1}^2 \quad {\dot{q}_2}^2\right]^T \\ \ddot{q} = \left[{\ddot{q}_1}^2 \quad {\ddot{q}_2}^2\right]^T \end{cases} \tag{B-5}$$

Injecting the expressions of the end effector's accelerations given in (B-4) into the formulation of the tangential contact force presented in (3-2), he following expression of the normal contact force can be deduced:

$$F_N(q,\dot{q},U) = g_1(q,\dot{q}) + g_2(q)U \tag{B-6}$$

Here, the following functions have been used:

$$\begin{cases} g_1(q,\dot{q}) = {B_1}^{-1}(f_1 + B_2 m_3 h_2\,\dot{q}^2)) \\ \qquad\qquad - {B_1}^{-1} B_2\left(m_3 g + F_f + h_1 {h_2}^{inv} h_1\,\dot{q}^2\right) \\ g_2(q) = {B_1}^{-1} f_2 \end{cases} \tag{B-7}$$

Appendix C: *frictional force formulation*

The frictional force that we have chosen to use depends on both the end effector velocity ($\dot{y}_3$) and charge (Γ_N), such as:

$$\begin{cases} F_f = (F_{cou} + F_{vis} + (F_s - F_c)\left(exp\left|\frac{\dot{y}_3}{v_s}\right|^{\gamma_s}\right) sign(\dot{y}_3))\,\frac{\Gamma_N}{\Gamma_0} \\ F_{cou} = F_c\, sign(\dot{y}_3) \\ F_{vis} = F_v\,\dot{y}_3 \end{cases} \tag{C-1}$$

Here, the definition of the following variables is needed:

- F_{cou} : Coulomb friction
- F_{vis}: Viscous friction
- F_s : static friction, necessary to begin a movement from a velocity null
- F_r: breaking force, making the transition from a velocity null (static friction) to a certain velocity (kinetic friction)
- Γ_N : Charge of the robot. It is proportional to the normal force
- Γ_0 : charge of the robot vacuum
- v_s : Stribeck speed (low speed)

- γ_s : Parameter affecting the slope of the Stribeck effect

Appendix D: ***weighting matrices formulation***

The hybrid control strategy is based on:

- A virtual reference model for the contact force regulation:

$$\ddot{x}_{3_d} - \Lambda_3 \dot{x}_{3_d} - \Lambda_4 \left(x_{3_d} - x_3 \right) = 0 \qquad \text{(D-1)}$$

The virtual weighting matrices $\mathbf{\Lambda_3}$ and $\mathbf{\Lambda_4}$ are defined with the ith pole of the end effector's virtual motion $\boldsymbol{s_i} < 0$, such as:

$$\begin{cases} \Lambda_3 = \sum_{i=1}^{n} s_i \\ \Lambda_4 = \prod_{i=1}^{n} s_i \\ n = 2 \end{cases} \qquad \text{(D-2)}$$

- A motion regulator's reference model:

$$\left(\ddot{y}_{3_d} - \ddot{y}_3 \right) - \Lambda_1 \left(\dot{y}_{3_d} - \dot{y}_3 \right) - \Lambda_2 \left(y_{3_d} - y_3 \right) = 0 \qquad \text{(D-3)}$$

The weighting matrices $\mathbf{\Lambda_1}$ and $\mathbf{\Lambda_2}$ are defined with the ith pole of the robotic system $\boldsymbol{p_i} < 0$ as follows:

$$\begin{cases} \Lambda_1 = \sum_{i=1}^{n} p_i \\ \Lambda_2 = \prod_{i=1}^{n} p_i \\ n = 2 \end{cases} \qquad \text{(D-4)}$$

References

[1] A. Mugan, A. G. Ulsoy and N. H. McClamroch, "Experimental Modeling of Robot Manipulators with Actuator Dynamics for Force and Motion Control", Proceedings of the IEEE International Workshop on Intelligent Motion Control, vol. 1, **(1990)**, pp. 313-319.
[2] G. Zeng and A. Hemami, "An overview of robot force control", Robotica, vol. 15, no. 5, **(1997)** , pp. 473-482.
[3] H. Hemami and B. Wyman, "Modeling and control of constrained dynamic systems with application to biped locomotion in the frontal plane," IEEE Transaction on Automatic Control, no. 4, **(1979)**, pp. 526–535.
[4] H. Hemami, "A general framework for rigid body dynamics, stability and control," Journal of Dynamic Systems, Measurement and Control, vol. 124, **(2002)**, pp. 241–251.
[5] J. J. Craig and M. H. Raibert, "A systematic method of hybrid position/force control of a manipulator", IEEE Computer Software and Applications Conference, vol. 1, **(1979)**, pp. 446-451.
[6] J. J. Craig and M. H. Raibert, "Hybrid position/force control of manipulators", ASME Journal of Dynamic Systems, Measurement and Control, vol. 102, **(1981)**, pp. 126-133.
[7] J. J. Gonzalez and G. R. Widmann, "A new model for nonlinear friction compensation in the force control of robot manipulators", IEEE International Publication, **(1997)**, pp. 201-203.
[8] J. K. Mills and A. A. Goldenberg, "Force and position control of manipulators during constrained motion tasks", IEEE Transactions on Robotics and Automation, vol. 5, no. 1, **(1989)**, pp. 30-46.
[9] J. S. Liu and S. L. Chen, "Robust hybrid control of constrained robot manipulators via decomposed equations", Journal of Intelligent and Robotic systems, Theory and applications, vol. 23, no. 1, **(1998)**, pp.45-70.
[10] K. Iqbal, H. Kallel and H. Hemami, "Linear decoupling controllers for constrained dynamic systems", International Journal of Control, vol. 60, no. 4, **(1994)**, pp. 607-616.
[11] R. Lozano and B. Brogliato, "Adaptive hybrid force-position control for redundant manipulators", IEEE Transactions on Automatic Control, vol. 37, no. 10, **(1992)**, pp. 1501-1505.
[12] S. Hayati, "Hybrid position/Force control of multi-arm cooperating robots", IEEE International Conference on Robotics and Automation, vol. 3, **(1986)**, pp. 82-89.

[13] T. Yoshikawa, "Dynamic hybrid position/force control of robot manipulators, Description of hand constraints and calculation of joint driving force", IEEE Journal of Robotics and Automation, vol. 3, no. 5, **(1987)**, pp. 386-392.
[14] Y. Zhou, "Dynamic model and force control for two manipulators handling a pin-jointed object", IEEE Conference on Decision and Control, vol. 3, **(1991)**, pp. 2763-2768.

Authors

Amine CHAÂBOUNI, was born in 1981 in Tunisia. He received the engineer diploma from the National Institute of Applied Science and of Technology, INSAT, in Tunisia. Since 2007 he is a research engineer and PhD student in Electrical Engineering at the Department of Physics and Electrical Engineering, INSAT, Tunisia.

Ines Belaïd Dlimi was born in 1982 in Tunisia. In 2007 she became an industrial computing and automic engineer at the department of Physics and Electrical Engineering within the National Institute of Applied Science and of Technology, INSAT, in Tunisia. In 2008 she obtained a master degree of industrial computing. Since, she is a PhD student in Electrical Engineering at INSAT.